Biological Control 218 (2026) 106073

Contents lists available at ScienceDirect

Biological Control

journal homepage: www.elsevier.com/locate/ybcon

Temperature-dependent shift in cyclic lipopeptide-mediated biocontrol of *Rhizoctonia solani* in bean by *Pseudomonas fuscovaginae* UPB0736

Bishnu Prasad Marahatta, Monica Höfte *

Lab of Phytopathology, Department of Plants and Crops, Faculty of Bioscience Engineering, Ghent University, Coupure Links 653, 9000 Ghent, Belgium

HIGHLIGHTS

- Temperature shapes the antifungal activity of *P. fuscovaginae* UPB0736
- Syringotoxin and fuscopeptin are essential CLPs for disease protection at 18 °C
- At 24 °C, UPB0736-mediated biocontrol is inconsistent
- Absence of syringotoxin and fuscopeptin unmasks an alternative mechanism at 28 °C

GRAPHICAL ABSTRACT

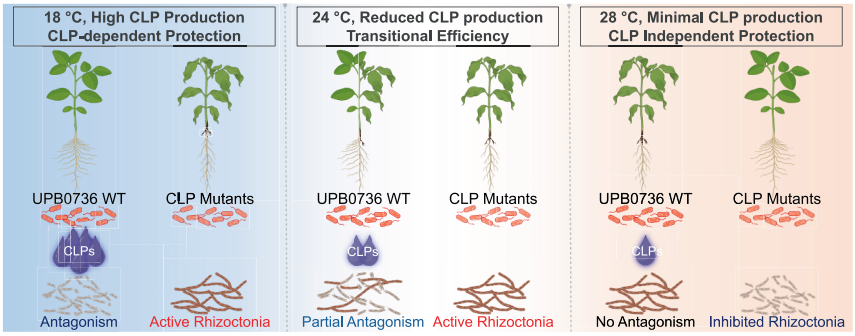

ARTICLE INFO

Keywords:
Cyclic lipopeptides
Fuscopeptin
Phaseolus vulgaris
Pseudomonas asplenii
Pseudomonas fuscovaginae
Syringotoxin
Temperature regulation

ABSTRACT

Understanding the mechanisms of microbial biocontrol is complex, as numerous biotic and abiotic factors can influence its function and effectiveness. In this study, the effect of temperature on the biocontrol efficiency of *Pseudomonas fuscovaginae* UPB0736 against *Rhizoctonia solani* (AG 5 and AG 2–2) in common bean (*Phaseolus vulgaris*) was studied. *P. fuscovaginae* UPB0736 produces two cyclic lipopeptides (CLPs) with antifungal activity against *R. solani*: syringotoxin (Mycin-type) and fuscopeptin (Peptin-type). Disease suppression was analyzed at three different temperatures (18 °C, 24 °C, and 28 °C) using the wild-type strain UPB0736 and knockout mutants impaired in the production of syringotoxin, fuscopeptin, or both CLPs.

This study describes a clear, temperature-dependent shift in the antifungal mechanism and efficiency *in planta* by UPB0736. At 18 °C, UPB0736 provided a consistent, CLP-dependent protection against *R. solani*. Notably, even removing a single CLP (either Mycin or Peptin) drastically reduced the efficacy. At 24 °C, effectiveness decreased, and biocontrol became inconsistent. At this intermediate temperature, the bacteria act as a preventive barrier protecting plants from early infection rather than curing an already established disease. At 28 °C, the wild-type surprisingly failed to provide protection, and contrastingly, the double knockout mutant significantly reduced disease. Root colonization remained constant across the entire temperature range. This confirms that the temperature-dependent variation in biocontrol was not caused by differences in root colonization, but rather by a complex temperature-dependent regulation of CLP production in the bacterial population.

* Corresponding author.
E-mail address: monica.hofte@ugent.be (M. Höfte).

https://doi.org/10.1016/j.biocontrol.2026.106073
Received 1 April 2026; Received in revised form 29 May 2026; Accepted 31 May 2026
Available online 1 June 2026

1. Introduction

Rhizoctonia, belonging to the phylum *Basidiomycota*, is a filamentous fungus unable to produce asexual spores (González García et al., 2006). *Rhizoctonia solani*, a facultative saprophyte with a broad host range (Bhuiyan et al., 2025), is known to infect more than 200 plant species, including rice, potatoes, soybeans, cereals, vegetables, and many other crops of high economic importance (Yang et al., 2022). It is the causal agent of many soilborne diseases (Ajayi-Oyetunde and Bradley, 2018). Infection and yield losses have also been reported in common bean production systems, making *R. solani* one of the economically important pathogens of this crop. Management of *R. solani* is challenging due to limited host resistance and its long-lasting survival structures, such as sclerotia. Therefore, identifying and applying sustainable biological control measures against *R. solani* are very important (Akber et al., 2023).

R. solani is a species complex as it constitutes different genetically diverse clusters, which are classified into distinct anastomosis groups (AGs) (Cubeta and Vilgalys, 1997). Grouping of strains into AGs depends on hyphal anastomosis or somatic compatibility, as well as differences in genetics, morphology, host range, biochemicals, and other life functions (Carling, 1996; Nandeesha et al., 2021; Sun et al., 2024). Anastomosis groups of *R. solani* can differ in virulence, host plant preference, and disease symptoms (Bolkan, 1985). In common beans, anastomosis group AG 2–2 is known to be associated with root rot and damping off (Godoy-Lutz et al., 2008; Nerey et al., 2010; Valentín Torres et al., 2016), while AG 5 has been reported to cause root and hypocotyl rot (Eken and Demirci, 2004) and root and stem rot (Canpolat et al., 2023).

Pseudomonas are rod-shaped, non-spore-forming, gram-negative bacteria belonging to the Phylum *Pseudomonadota*. *Pseudomonas* is a large genus with more than 260 described species, divided into groups and subgroups. *Pseudomonas fluorescens*, the largest group, comprising 11 subgroups (Girard et al., 2021), harbors numerous plant-beneficial soil-inhabiting bacteria with biocontrol and biostimulation capabilities (Höfte, 2021). They produce a range of bioactive metabolites. Among these metabolites, cyclic lipopeptides (CLPs) are compounds of significant importance, as they have been studied for their roles in pathogenicity and biological control (Girard et al., 2020), as well as for various other functions, such as mobility, biofilm production, and antimicrobial activity (Geudens and Martins, 2018; Götze and Stallforth, 2020; Oni et al., 2022).

CLPs are composed of an oligopeptide, which forms a macrocyclic ring, linked to a fatty acid tail, and are produced via Non-Ribosomal Peptide Synthetases (NRPSs) (Ballio et al., 1990; Geudens and Martins, 2018; Raaijmakers et al., 2010). Dissimilarities in the length and configuration of the fatty acid tail, as well as the length, configuration, and composition of amino acids in the oligopeptide, give rise to different CLPs (Malfanova et al., 2012; Raaijmakers et al., 2010). *Pseudomonas* CLPs are currently classified into 17 different families, further grouped into three clusters: the negatively charged Acidilins, the positively charged Peptins, and the ambivalent Mycins, which carry both acidic and basic amino acids (Kovács et al. 2025). CLPs have a wide range of vital applications, from human and plant health to biotechnology and industry, but their utilization is hampered by limited production and low yields. In *Pseudomonas*, various factors, including temperature, pH, aeration, nutrient availability, and plant signals, can influence CLP production (Bender and Scholz-Schroeder, 2004; Nybroe and Sørensen, 2004; Raaijmakers et al., 2006). *Pseudomonas* species that produce cyclic lipopeptides (CLPs) are widely recognized and studied for their ability to suppress soilborne pathogens (Oni et al., 2022). However, there remains a significant research gap regarding how environmental factors influence the effectiveness of CLP-based biocontrol.

Pseudomonas fuscovaginae (also called *P. asplenii*) belongs to the *P. asplenii* subgroup within the *P. fluorescens* group (Girard et al., 2020; Hesse et al., 2018; Miyajima et al., 1983; Tohya et al., 2020). The species was first described in Japan in 1976 and causes brown sheath rot in rice (Tanii et al., 1976; Tohya et al., 2020). *P. fuscovaginae* UPB0736 was isolated from sheath rot-infected rice plants from the dry highlands of Madagascar (Duveiller et al., 1990; Patel et al., 2012). It is known to produce three CLPs: syringotoxin (Ballio et al., 1990), fuscopeptin (Ballio et al., 1996), and asplenin (Ferrarini et al., 2022). Although pathogenic on rice sheaths, Ferrarini et al. (2022) found that *P. fuscovaginae* UPB0736 demonstrates strong CLP-mediated antifungal effects against *R. solani in vitro*, suggesting its potential as a model to study the antifungal role of CLPs *in planta*.

Syringotoxin is a low-molecular-weight lipodepsipeptide belonging to the Mycin CLP family, reported in *P. fuscovaginae* and *P. syringae* (Ballio et al., 1990; Lavermicocca et al., 1997). It is known for its amphiphilic properties, resulting from the amphipathic nature of the peptide head and the hydrophobic fatty acid tail, which enables it to exhibit surfactant properties. It consists of a 9-amino acid macrolactone ring with a 14-carbon 3-hydroxy fatty acid tail. Fuscopeptin, on the other hand, belongs to the Peptin family and has two forms- A and B, based on the length of its fatty acid chain. Fuscopeptin A has an 8-carbon chain, while Fuscopeptin B has a 10-carbon chain. Fuscopeptin consists of 19 amino acids, of which five are involved in the lactone ring. Syringotoxin and fuscopeptin can be phytotoxic, but also exhibit strong antifungal activity against various phytopathogens, including *R. solani* (De Rop et al., 2025; Ferrarini et al., 2022; Weeraratne, 2018; Weeraratne et al., 2020). Asplenin is a 13-amino acid containing CLP with 8-amino acids composing the ring. Asplenin exhibits no antimicrobial activity but plays a significant role in swarming mobility (Ferrarini et al., 2022) (Table 1).

In a recent study using *P. fuscovaginae* UPB0736, De Rop et al. (2025) aimed to optimize its antifungal activity and observed a considerable influence of temperature on CLP production. In an *in vitro* environment, syringotoxin and fuscopeptin production and antifungal activity were higher at lower temperatures; however, the role of these metabolites in a tripartite interaction (plant–fungus–bacterium) remains unclear.

This study aims to evaluate the *in planta* antifungal effect of UPB0736 against *R. solani* (AG 5 and AG 2–2) at different temperatures. The main research objective is to understand the roles of syringotoxin (Mycin) and fuscopeptin (Peptin) in biocontrol, and whether the roles of these CLPs change with temperature. It is hypothesized that in UPB0736, *in planta* biocontrol is strictly CLP-mediated, and its disease-protection efficiency will decrease with increasing temperature because CLP production declines with higher temperatures.

2. Materials and methods

2.1. Microbes and microbial growth

Luria-Bertani Agar (LBA) and King's B Agar (KBA) plates were used for culturing *Pseudomonas*, while Potato Dextrose Agar (PDA) was used for growing *Rhizoctonia*. For overnight cultures, Luria-Bertani (LB) broth was employed. For long-term storage of bacteria, 500 μL of an overnight-grown culture, incubated at 28 °C for 24 h with shaking, was mixed with 500 μL of sterile 40% glycerol in a cryovial and stored at −80 °C. For long-term storage of *Rhizoctonia*, five mycelial plugs of 4-day-old *Rhizoctonia*, incubated at 28 °C on PDA plates, were combined with 750 μL of skim milk and 750 μL of 40% sterile glycerol, and stored at −80 °C.

2.2. In vitro tests and IC_{50} determination

Dual cultures were performed on one-fifth-strength PDA plates. Initially, an overnight bacterial culture was prepared in LB or KB broth at 28 °C and 150 rpm, and *Rhizoctonia* was grown in PDA at 28 °C for 4 days. Two 10 μL drops of *Pseudomonas* were placed 4 cm apart, with a 3 mm pathogen mycelial plug at the center of the plate, and the plate was incubated at 18, 24, or 28 °C. The results were recorded after 5 days of incubation by measuring the mycelium inhibition using ImageJ

software. The Percentage Area Inhibition (PAI) value was calculated as follows.

$$Percentage\,Area\,inhibition(PAI) = \frac{Colony\,Area\,of\,Control - Colony\,Area\,of\,Treatment}{Colony\,Area\,of\,Control} \times 100\%$$

For IC_{50} determination of *P. fuscovaginae* UPB0736 supernatant against *R. solani* AG 2–2 and AG 5, the bacterial strain was cultured in 200 mL of KB liquid medium in a 1 L baffled flask and incubated at 150 rpm for 28 h at 18 °C. The supernatant was filter-sterilized and combined with PDA in different ratios. A 3 mm mycelial plug of *R. solani* was placed at the center of each Petri dish and incubated at temperatures of 18 °C or 28 °C. Fungal growth was subsequently measured after 48 h and 24 h, respectively, and the extent of mycelium inhibition was evaluated. The half-maximal effective dose (ED_{50}, mL), defined as the volume of *P. fuscovaginae* UPB0736 cell-free supernatant required to achieve 50% inhibition of fungal growth, was determined. The corresponding half-maximal inhibitory concentration for syringotoxin (IC_{50}, mg/L) was calculated by converting ED_{50} values to concentrations of chemically quantified bioactive metabolites, following the methodology described by De Rop et al. (2025).

2.3. Plant bioassay

Antagonistic bioassays were conducted using *Phaseolus vulgaris* L. cv. Prelude (Sluis Garden Company, Netherlands). Plants were grown in plastic trays measuring 22 × 15 × 6 cm^3, filled with 700 g of 1:1 (w/w) non-sterilized "professional universal soil Type 1" potting soil (Structural Company: dry matter = 25%; organic matter = 20%, and pH = 5–6.5), and washed sand (Cobogarden). Bean seeds were first surface-sterilized in 1% sodium hypochlorite for 2 min, thoroughly rinsed with sterile water, and then allowed to pre-germinate on sterile, moist filter paper and cotton in petri plates. These plates were incubated in the dark at 28 °C for 3 days. *Pseudomonas* strains were first grown overnight on KBA plates at 28 °C, washed, and diluted to 10^6 Colony-forming units (CFU) in 250 μL of 0.85% (w/v) saline solution. These bacterial suspensions were used to introduce bacteria: first by dipping pregerminated bean seeds (bean seedlings) in the suspension for 2 min before sowing, and later by thoroughly mixing the suspension with the growth substrate. Ten pre-germinated bean seedlings, after root dipping in bacteria, were sown in each tray in two rows (6 cm apart). The trays were kept in a growth chamber with 60% relative humidity, a 16/8 h day/night light cycle, and at temperatures of 18, 24, or 28 °C.

R. solani inoculum for both AG 5 and AG 2–2 was prepared by inoculating sterile wheat kernels (overnight soaking followed by autoclaving two times on consecutive days) with five 5-mm PDA plugs from a 3-day-old fungal culture, and incubated at 28 °C for 9 days with intermittent shaking. Pathogen inoculation was done by placing 40 *R. solani*-infected kernels in the midline of two seedling rows at a depth of 2 cm, 3 days after transplanting bean seedlings in the trays. Disease severity of the infected plants was recorded when the second trifoliate leaf emerged, which occurred 14, 11, and 7 days post-infection for plants grown at 18, 24, and 28 °C, respectively, by carefully uprooting, washing, and evaluating disease symptoms (Fig. 1).

The experimental design involves a series of independent bioassays. Initial screenings were conducted at 24 °C to assess the consistency of *R. solani* AG 2–2 pathogenicity. Then, a standardized protocol was established using *R. solani* AG 5 at 18 °C and 24 °C, and *R. solani* AG 2–2 at 28 °C to ensure optimal disease pressure across the temperature range. For the final comparative analysis of the wild-type UPB0736 and its CLP mutants (Table 2), experiments at 18 °C and 28 °C were carried out in two separate temporal repetitions, while those at 24 °C were conducted once. Each treatment within an experiment included three replicate trays with 10 plants per tray, resulting in 30 to 60 plants per treatment at each temperature setpoint. Disease Severity Index (DSI) values were calculated and compared using the following formula.

$$Disease\,Severity\,Index(DSI) = \frac{\sum(Class\,value \times Class\,frequency)}{Total\,number\,of\,plants \times Maximum\,possible\,class\,value} \times 100\%$$

2.4. Root colonization assay

For the root colonization assay, five roots per treatment were randomly selected, cleaned, air-dried, and weighed. Each root was ground in 10 mL of 0.85% (w/v) sodium chloride solution and half a tablespoon of sterile sand using a sterile mortar and pestle. Thus-obtained homogenates were serially diluted up to 10^{-6}, and 100 μL of 10^{-5} and 10^{-6} suspensions were cultured in freshly prepared KBA plates. The plates were incubated at 28 °C for 24 h, and the number of

Table 1
Cyclic lipopeptides (CLPs) produced by *P. fuscovaginae* UPB0736 and their chemical structures.

CLPs	Structure	References
Syringotoxin	C14-OH **L-Ser–D-Dab–Gly–D-Hse–L-Orn–L-αThr–Z-Dhb–L-AspOH–L-ThrCl**	Ballio et al., 1990; Ferrarini et al., 2022
Fuscopeptin A	C8-OH Dhb–D-Pro–L-Leu–D-Ala–D-Ala–D-Ala–D-Ala–D-Val–Gly–D-Ala–D-Val–D-Ala–D-Val–Dhb**–D-αThr–L-Ala–L-Dab–D-Dab–L-Phe**	Ballio et al., 1996
Fuscopeptin B	C10-OH Dhb–D-Pro–L-Leu–D-Ala–D-Ala–D-Ala–D-Ala–D-Val–Gly–D-Ala–D-Val–D-Ala–D-Val–Dhb**–D-αThr–L-Ala–L-Dab–D-Dab–L-Phe**	Ballio et al., 1996
Asplenin	C10-OH Leu–Glu–Leu–Val–Gln**–Ser–Val–Leu–Ser–Leu–Leu–Ser–Val**	Ferrarini et al., 2022

Note: Structure describes the carbon count and composition of Amino Acids (AAs). The amino acids in bold compose the lactone ring structure of the CLPs.

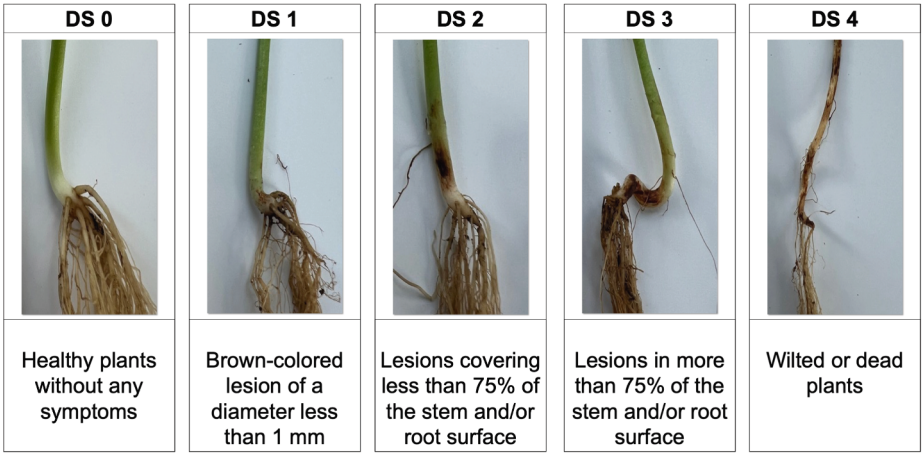

Fig. 1. Disease severity scale ranging from DS0 to DS4 used to evaluate root rot symptoms caused by *Rhizoctonia* spp. in bean plants.

Table 2
Fungal and bacterial strains used in the study, along with their characteristics and origins.

Microorganism	Strains	Characteristics	References
Fungi	*R. solani* AG 5 strain RhCaES-62	Brown wilted stem bases/ leaves in carrot, Sweden	Marcou et al., 2021
	R. solani AG 2–2 strain CuHav-Rs18	Root rot in beans in Cuba	Nerey et al., 2010
Bacteria	*P. fuscovaginae* UPB0736	Sheath rot on rice in Madagascar	Patel et al., 2012
	UPBΔM (also called UPB0736-Δ*fst*)	Syringotoxin mutant of *P. fuscovaginae* UPB0736, deletion in the *fstA* gene	Ferrarini et al., 2022
	UPBΔP (also called UPB-Δ*fus*)	Fuscopeptin mutant of *P. fuscovaginae* UPB0736, deletion in the *fusA* gene	Ferrarini et al., 2022
	UPBΔMΔP (also called UPB-Δ*fst*-Δ*fus*)	Syringotoxin and Fuscopeptin mutant of *P. fuscovaginae* UPB0736, deletion in the *fstA* and *fusA* gene	Ferrarini et al., 2022

colonies developed per plate was enumerated based on morphological characteristics and fluorescence visualization under UV light.

2.5. Statistical analysis

Microsoft Excel (version 16.105) was used to collect data and perform preliminary visualization. Data were analyzed in RStudio (Version 2024.04.1 + 748) at the 95% confidence level for all analyses. Continuous variables, such as fungal growth area (cm^2), were analyzed using a three-way analysis of variance (ANOVA) followed by Tukey's Honestly Significant Difference (HSD) post hoc test ($p < 0.05$). R packages such as "emmeans", "multcomp", and "ggplot2" were used for statistical analyses and visualizations.

Dose–response relationships between supernatant volume and percentage area inhibition (PAI) were analyzed in RStudio using the "drc" package. A three-parameter log-logistic model was fitted to the data, and the half-maximal effective dose (ED_{50}) and its 95% confidence interval were estimated using the delta method.

The variable used to analyze disease severity, disease scale (DS), is a categorical ordinal variable. First, the potential effects of tray and experiment were assessed using Kruskal-Wallis H tests within each treatment to ensure the model was correctly specified for statistical analysis. The significance tests for disease severity analyses were first done using the non-parametric Kruskal-Wallis H test. For post hoc analysis, the Pairwise Wilcoxon rank-sum test with Benjamini-Hochberg (BH) correction was used.

To further analyze treatment effects across disease severity thresholds, cumulative link models (CLMs) with a logit link were fitted using the "ordinal" package in R at each temperature point. The treatment effects were quantified using the model coefficient (β) and the corresponding odds ratio ($OR = e^{\beta}$). The proportional odds (PO) assumption was first examined using a nominal effects test for treatment and experiment factor. When the PO assumption was satisfied, standard CLMs were used, but if the assumption was violated, partial proportional odds (PPO) models with a logit link were fitted for comparison, and if treatment effect estimates were stable and consistent between the PO and PPO models, the more parsimonious PO model was selected for final reporting. The predicted probabilities of healthy plants and/or successful disease control, denoted as "Health Probabilities", are the cumulative probabilities of plants remaining in disease severity classes DS0 or DS1. It was calculated using the "predict" function for the fitted cumulative link models. These probabilities represent the model-adjusted likelihood of successful biocontrol, accounting for both treatment effects and experimental variation in treatments containing BCA, but for pathogen control, they represent the baseline probability of healthy plants.

Finally, a global cumulative link model (CLM) was constructed by pooling data across 18, 24, and 28 °C to examine the interaction between temperature and bacterial treatment. In this analysis, the two *R. solani* anastomosis groups (AG 5 and AG 2–2) were treated collectively as a single pathogen factor, so that the model reflected the overall effect of the bacterial treatments on the pathogen regardless of anastomosis groups. The significance was tested using the Likelihood Ratio Test via the "nominal test" function in Rstudio. Post-hoc comparisons were done using the "emmeans" package with Tukey's HSD adjustment. Health Probabilities were also calculated and analyzed for this global cumulative link model.

3. Results

As reported previously, *P. fuscovaginae* UPB0736 shows CLP-mediated antagonism against *R. solani* AG 2–2 *in vitro* (De Rop et al., 2025; Ferrarini et al., 2022). However, translating this antagonistic activity to a complex *in planta* rhizosphere environment remains a significant challenge for any BCA. To evaluate how UPB0736 behaves *in planta*, a series of plant assays was conducted at 24 °C using common bean plants. This temperature was selected as a baseline representing ideal growth conditions for host, fungus, and bacterium.

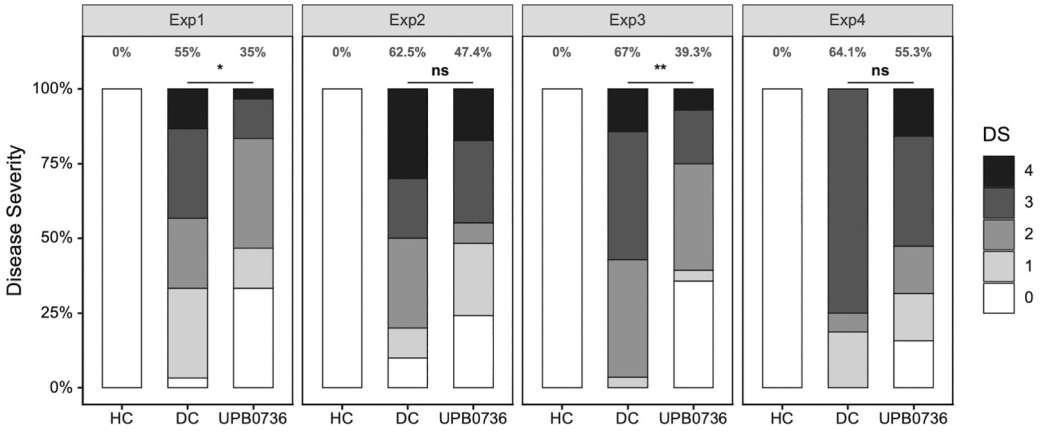

Fig. 2. Percentage stacked bar plot displaying the distribution of disease severity across treatments in four initial experiments using *R. solani* AG 2–2 and *P. fuscovaginae* UPB0736 at 24 °C. Bars represent the proportion of plants in each disease scale (DS), from healthiest (DS0) to most diseased (DS4). Each treatment is displayed as 100% stacked bars. Each facet corresponds to a different experiment. Above each plot, asterisk signs indicate Pairwise Wilcoxon significance between positive disease control (DC) and UPB0736 ($p \geq 0.05$ = ns; $0.01 \leq p < 0.05$ = *; $0.001 \leq p < 0.01$= **). The Disease Severity Index (DSI, %) is shown above each treatment group. Statistical analyses were performed using Kruskal-Wallis tests and Pairwise Wilcoxon rank-sum tests with Benjamini–Hochberg correction for each experiment (n = 30 plants per treatment). HC represents the healthy control (non-inoculated plants).

3.1. UPB0736 biocontrol at 24 °C

The biocontrol effectiveness of *P. fuscovaginae* UPB0736 against *R. solani* AG 2–2 was inconsistent at 24 °C. Disease severity differed significantly among treatments across all experiments (Kruskal–Wallis, $p < 0.0001$; Table S1). The effect of UPB0736 compared to the positive disease control was significant in Experiment 1 ($p = 0.0150$) and Experiment 3 ($p = 0.0016$), but no significant reduction in disease was observed in Experiment 2 ($p = 0.1200$) and Experiment 4 ($p = 0.5000$) (Fig. 2).

To resolve these inconsistencies, a cumulative link model (CLM) with a logit link was fitted, excluding the healthy control group. The model suggested a significant overall reduction in disease with UPB0736 ($p < 0.0001$), as plants treated with UPB0736 had a 64% higher probability of being in a lower disease category than plants in the positive pathogen control. However, the proportional odds assumption was violated ($p = 0.0119$), suggesting that the efficiency of UPB0736 varied across severity thresholds (Table S2).

To account for this violation, a partial proportional odds (PPO) model was fitted, allowing treatment effects to vary across disease transitions, revealing that the effect of UPB0736 is strongest at the lowest threshold (between DS0 and DS1) and progressively weaker at higher thresholds. This means that UPB0736 primarily prevents early disease progression rather than reducing disease severity (Table S2).

The inconsistent biocontrol effectiveness by UPB0736 indicated that the protection may be sensitive to environmental or physiological conditions. To test the influence of temperature, subsequent experiments were conducted at 18 °C and 28 °C. Nonetheless, performing *in planta* bioassays at the proposed new temperatures required fungal pathogens that exert sufficient disease pressure under these conditions. Therefore, a pathogenicity screening *in planta* was carried out using two *R. solani* AGs: AG 5, originating from a temperate region (Sweden), and AG 2–2, originating from a tropical region (Cuba).

3.2. Temperature-dependent pathogenicity of R. solani

Pathogenicity of *R. solani* varied markedly with temperature and anastomosis groups. For all three temperatures (18 °C, 24 °C, and 28 °C), there was a significant difference in disease severity between treatments (all Kruskal–Wallis $p < 0.0001$; Table S3).

At 18 °C, AG 5 was pathogenic, whereas AG 2–2 failed to induce disease symptoms and did not differ from the healthy control ($p =$

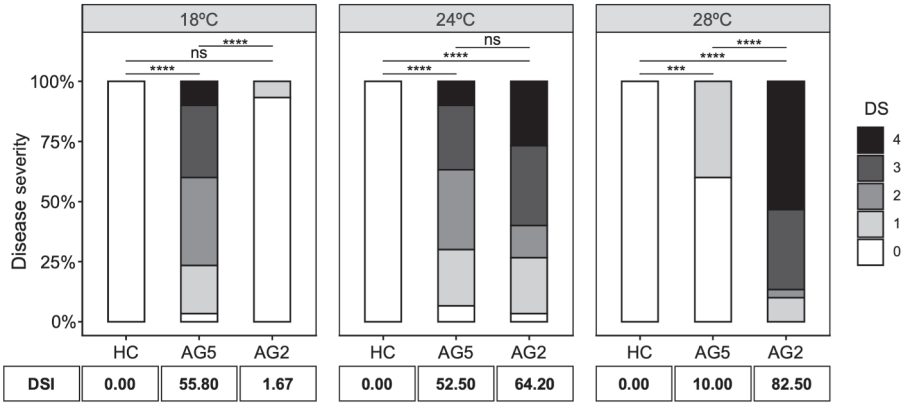

Fig. 3. Pathogenicity of *R. solani* is dependent on temperature and Anastomosis Groups (AGs). Stacked bar charts show the percentage distribution of disease severity in bean plants under different treatments at three temperatures (18 °C, 24 °C, and 28 °C), using two *R. solani* anastomosis groups (AG 5 and AG 2–2). Disease severity classes are ordinal, ranging from DS0 (no disease symptoms) to DS4 (severely diseased). The disease severity index (DSI) is displayed at the bottom of the plot for each treatment. Statistical differences among treatments within each temperature were assessed using Kruskal-Wallis tests, followed by pairwise Wilcoxon rank-sum tests with Benjamini–Hochberg correction for multiple comparisons. Significance levels are indicated as follows: $p \geq 0.05$ (ns); $p < 0.001$ (***); and $p < 0.0001$ (****). HC represents the healthy control (non-inoculated plants).

0.1610). In contrast, at 28 °C, AG 2–2 caused severe disease symptoms, whereas AG 5, although significantly different from the healthy control ($p < 0.0001$), exhibited minimal virulence with a DSI of only 10. Both anastomosis groups, however, caused disease in bean plants at 24 °C, and the difference in disease pressure between them was non-significant ($p = 0.1170$) (Table S3). Overall, *R. solani* AG 5 demonstrated reduced virulence with increasing temperature, whereas virulence increased for *R. solani* AG 2–2 (Fig. 3).

Since 18 °C is suboptimal for AG 2–2 and 28 °C is suboptimal for AG 5, these temperature-pathogen combinations were excluded from subsequent biocontrol experiments. However, before assessing biocontrol effectiveness *in planta*, it was crucial to determine to what extent UPB0736 and its CLP mutants exhibited antagonistic activity against these specific AGs under the proposed new temperature conditions.

3.3. In vitro activity against R. solani anastomosis groups

Antagonistic activity of *P. fuscovaginae* UPB0736 against *R. solani* depended on the specific combination of bacterial strains, temperature, and pathogen anastomosis group. A three-way ANOVA confirmed this, showing highly significant main effects of bacterial treatment, temperature, and pathogen on fungal mycelial growth area (all $p < 0.0001$), as well as significant two-way interactions and three-way interactions (all $p < 0.0001$; Table S4).

The UPB0736 wild-type (UPBWT) and fuscopeptin mutant UPBΔP exhibited comparable inhibition against *R. solani* AG 5 at 18 °C (40.36% and 39.60% PAI, respectively), which declined significantly as the temperature increased, reaching 16.75% and 21.70% PAI at 28 °C, respectively. Notably, both the syringotoxin mutant UPBΔM and the double mutant UPBΔMΔP exhibited very low or no antagonistic activity against AG 5 at all temperatures. The inhibitory activity of UPB0736 and its mutants against *R. solani* AG 2–2 was, in general, more robust and stable. The UPB0736 wild-type showed maximum suppression with 73.65% PAI at 18 °C, and 43.26% at 28 °C. The UPBΔP mutant consistently exhibited the second-highest efficacy across all temperatures, whereas both UPBΔM and UPBΔMΔP maintained low but significant inhibitory activity against AG 2–2 (Fig. 4).

The supernatant of *P. fuscovaginae* UPB0736 showed a distinct dose-dependent inhibition of both anastomosis groups, with AG 2–2 being consistently more sensitive than AG 5. At 18 °C, deduced IC_{50} values were 0.08 mg/L for AG 2–2 and 0.11 mg/L for AG 5, whereas at 28 °C, IC_{50} was 0.09 mg/L for AG 2–2 and 0.14 mg/L for AG 5 (Table S5). Building on these *in vitro* results and previous studies on AG 5 and AG 2–2, subsequent bean plant bioassay experiments were conducted at different temperatures to examine how UPB0736 expresses biocontrol *in planta*. It should be noted that in the absence of *R. solani*, inoculation with *P. fuscovaginae* UPB0736 or its CLP-mutants induced no phytotoxic symptoms in bean plants across all temperatures, yielding healthy plants (DS0). This confirms that observed disease symptoms were exclusively *R. solani*-derived and that UPB0736 is non-pathogenic to common bean under these conditions.

3.4. Biocontrol at low temperature (18 °C)

At 18 °C, *R. solani* AG 5 caused significant root and crown rot in beans. Co-inoculation with *P. fuscovaginae* UPB0736 wild-type significantly reduced disease severity in both repeats ($p < 0.0001$) while the UPB0736 mutants lacking syringotoxin (UPBΔM), fuscopeptin (UPBΔP), or both CLPs (UPBΔMΔP) did not significantly decrease disease in either repeat (all $p > 0.05$; Table S6). Bacterial colonization of the root tissue, measured as log CFU/g, ranged from 7.50 to 7.94, with no significant differences between UPB0736 wild-type and its mutant strains (Fig. 5).

To statistically confirm the observations, a cumulative link model with a logit link was applied by combining two experiments and removing the healthy control. No violation of the proportional odds assumption was detected for either treatment factor ($p = 0.2417$) or experiment factor ($p = 0.4987$) (Table S7). In this full model, UPB0736 wild-type was the only treatment to exhibit significant disease reduction against *R. solani* AG 5 ($\beta = -1.845$; $p < 0.0001$), with an approximately 84% reduction in the odds of moving to higher disease categories (OR = 0.16). Post-hoc Tukey-adjusted comparisons confirmed that UPBWT significantly protected plants from disease ($p < 0.0001$), whereas all other mutant strains were not significant (all $p > 0.05$). This efficacy was further reflected in the predicted probability of successful disease control (Health Probability) of 61–64% for wild-type versus 18–21% for UPBΔMΔP (Table S8A).

3.5. Biocontrol at moderate temperature (24 °C)

At 24 °C, both *R. solani* AG 5 and AG 2–2 caused significant root and crown rot symptoms in bean plants. In individual experimental trials, co-inoculation with *P. fuscovaginae* UPB0736 wild-type did not significantly reduce disease severity against either AG 5 ($p = 0.1309$) or AG 2–2 ($p = 0.2273$). Similarly, all mutants (UPBΔM, UPBΔP, and UPBΔMΔP) failed to significantly reduce disease severity compared with the pathogen control in either experiment (all $p > 0.05$) (Table S6). However, UPBWT was the only strain exhibiting a low DSI value, which indicates a partial, yet statistically unconfirmed, biocontrol effect of UPB0736 against both pathogen anastomosis groups. Bacterial colonization of root tissue, measured as log CFU/g, was consistent among wild-type and mutant strains, ranging from approximately 7.53 to 7.78 log CFU/g (Fig. 6).

To evaluate overall biocontrol efficacy and resolve the observed inconsistencies at 24 °C, data from both experimental repeats were pooled, with AG 5 and AG 2–2 treated as a single pathogen. A cumulative link model (CLM) with a logit link was fitted and analyzed. Although the proportional odds assumption for treatment ($p = 0.6775$) was fully satisfied, the experiment factor exhibited a violation ($p = 0.0026$; Table S7). Comparison of this standard model with the partial proportional odds (PPO) model, in which the experiment was treated as a nominal factor, yielded nearly identical treatment estimates. Since the inference regarding treatment effects stayed consistent and the improvement in model fit was minimal, the simpler proportional odds model was retained for final analysis.

In this model, UPBWT was associated with a significant reduction in disease severity relative to the pathogen control ($\beta = -0.853$; $p = 0.0104$), representing a 57% reduction in the odds of reaching higher disease severity categories (OR = 0.43). This finding contrasted with the non-significant results observed during non-parametric tests for the non-pooled data. However, the post hoc pairwise comparisons (Tukey-adjusted) indicated that the protection by the UPB wild-type was fragile, as it was on the threshold of significance compared to the pathogen control ($p = 0.0778$), but offered significantly superior protection as compared to UPBΔMΔP ($p = 0.0341$). The predicted probability of successful disease control (Health Probability) for UPB wild-type was moderate, ranging from 41.4% to 48.7% (Table S8B).

3.6. Biocontrol at high temperature (28 °C)

At 28 °C, *R. solani* AG 2–2 caused severe root and crown rot in bean plants. Co-inoculation with *P. fuscovaginae* UPB0736 wild-type in both repeats showed a marginal but non-significant reduction in disease severity as compared to the pathogen control (both $p > 0.05$). UPB0736 mutants lacking CLP production, however, showed different outcomes as compared to 18 °C and 24 °C. In replicate A, the double mutant (UPBΔMΔP) showed significantly less disease ($p = 0.0422$), while in replicate B, both UPBΔP and UPBΔMΔP significantly reduced disease ($p = 0.0178$ and $p = 0.0143$, respectively) (Table S6). Bacterial colonization of root tissue was consistent across treatments in both repeats, with population densities ranging from approximately 7.32 to 7.88 log CFU/g (Fig. 7).

To validate this observed difference, a cumulative link model with a

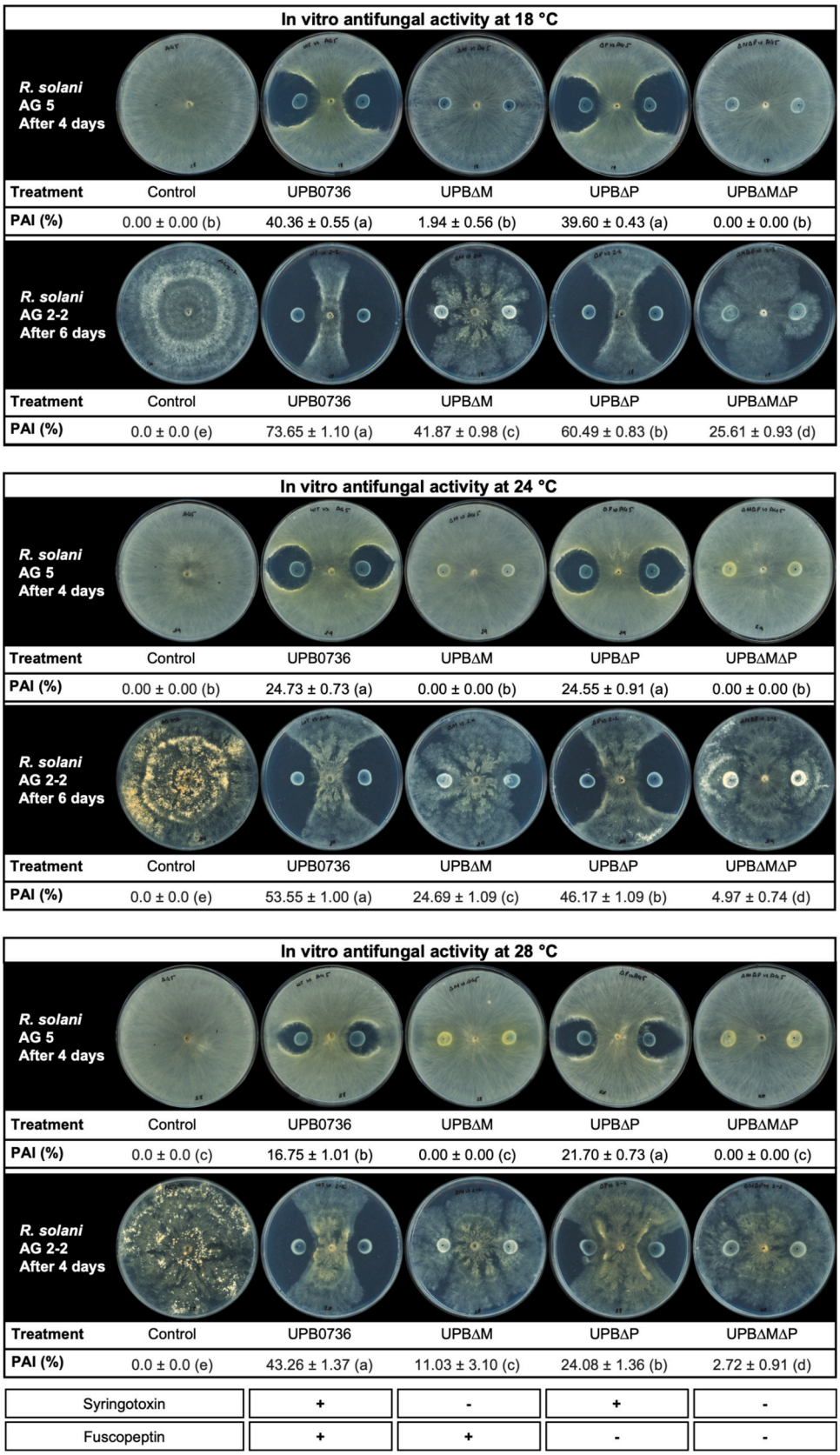

Fig. 4. *In vitro* dual-culture antifungal activity of *P. fuscovaginae* UPB0736 and its mutants against *R. solani* AG 5 and AG 2–2 at 18 °C, 24 °C, and 28 °C in one-fifth PDA. The panels display representative plates corresponding to each treatment combination, while the "control" represents uninhibited fungal growth. Values below each plate represent the mean Percentage Area Inhibition (PAI) ± standard deviation (n = 3). Letters in parentheses indicate statistical groupings based on mycelial growth area (cm^2). Treatments sharing the same letter within a specific pathogen-temperature combination are not significantly different (Three-way ANOVA, Tukey's HSD, $p < 0.05$). Symbols (+/−) denote the presence or absence of secondary metabolites in each strain.

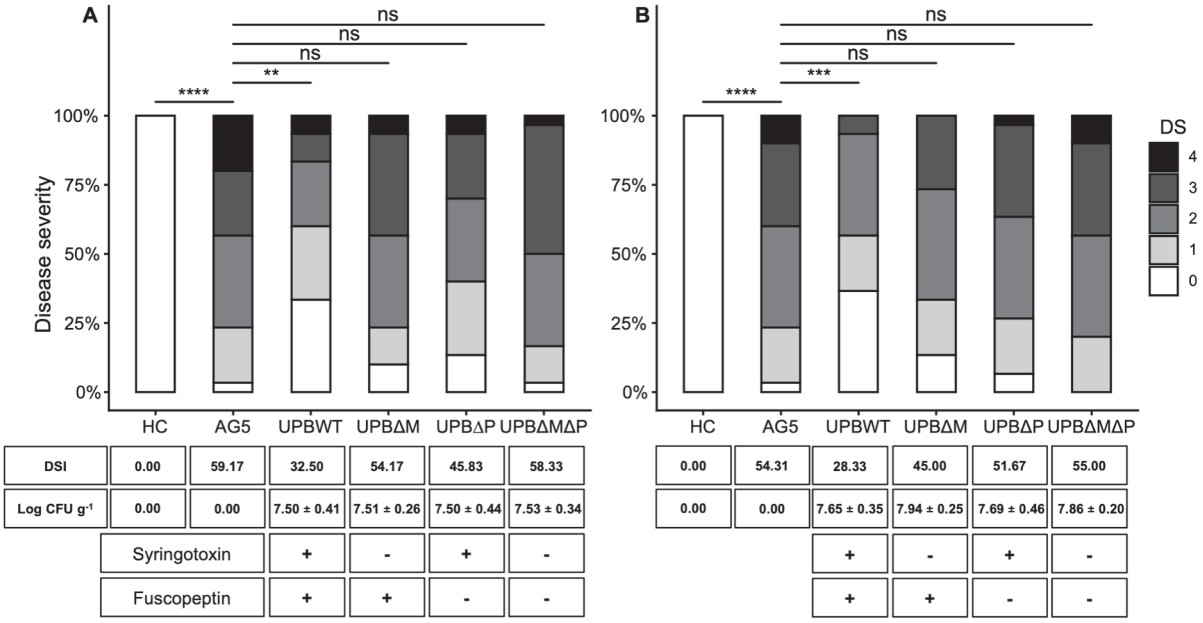

Fig. 5. Biocontrol of *R. solani* AG 5 by *P. fuscovaginae* UPB0736 and its CLP mutants in bean plants at 18 °C. Stacked bar charts show the percentage distribution of disease scales (DS0 – DS4) for each treatment (n = 30 plants per treatment) across two independent experiments (A and B). Disease severity index (DSI) and bacterial colonization (log CFU/g of root tissue) values are displayed at the bottom of the plot for each treatment. Kruskal-Wallis tests indicated significant differences among treatments (for both A and B: Kruskal-Wallis $p < 0.0001$; Table S6). Significance levels shown on top of the plots indicate Pairwise Wilcoxon significance with Benjamini-Hochberg correction between positive disease control (AG 5) and all other treatments ($p \geq 0.05$ = ns; $0.001 \leq p < 0.01$ = **; $0.0001 \leq p < 0.001$ = ***; and $p < 0.0001$ = ****). No significant tray effect was observed in either repeat. HC represents the healthy control (non-inoculated plants).

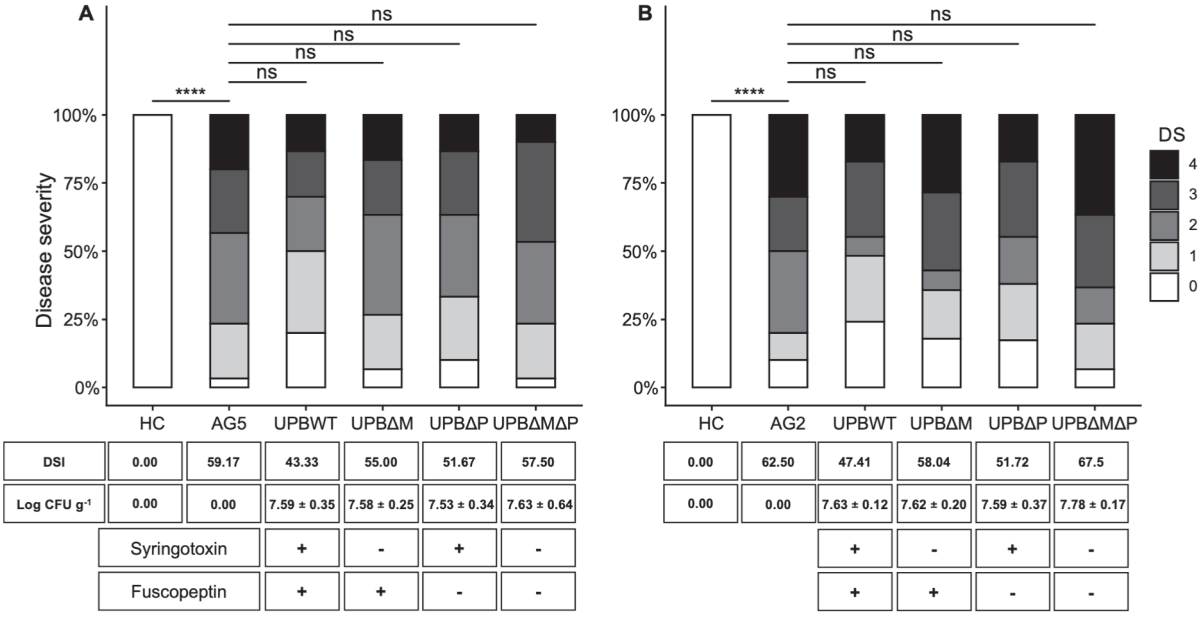

Fig. 6. Biocontrol of *R. solani* AG 5 (A) and AG 2–2 (B) by *P. fuscovaginae* UPB0736 (UPBWT) and its CLP mutants in bean plants at 24 °C. Stacked bar charts show the percentage distribution of disease scales (DS0 – DS4) for each treatment (n = 30 plants per treatment) across two separate experiments. Disease severity index (DSI) and bacterial colonization (log CFU/g of root tissue) values are indicated below the plots for each treatment. Kruskal-Wallis tests showed significant differences among treatments in both experiments (Kruskal-Wallis $p < 0.0001$; Table S6). Significance levels above the plots represent pairwise Wilcoxon rank-sum tests with Benjamini-Hochberg correction comparing positive disease controls (AG 5 for plot A and AG 2–2 for plot B) against all other treatments ($p \geq 0.05$ = ns and $p < 0.0001$ = ****). No significant tray effects were observed in either experiment. HC represents the healthy control (non-inoculated plants).

logit link was fitted on the pooled data of the two repeats. Model diagnostics for this pooled data indicated fulfillment of the PO assumption for the treatment factor ($p = 0.8564$) but significant violation for the experiment factor (nominal test: $p = 0.0009$). To account for this, a partial proportional odds (PPO) model was fitted, allowing the effect of the experiment factor to vary across response thresholds while keeping the treatment effect to satisfy the PO assumption. Although the PPO model provided a superior fit compared to the standard CLM (ΔAIC = 10.33), the improvement was minimal for treatment estimates. Hence, a simpler standard PO model was used for reporting (Table S7).

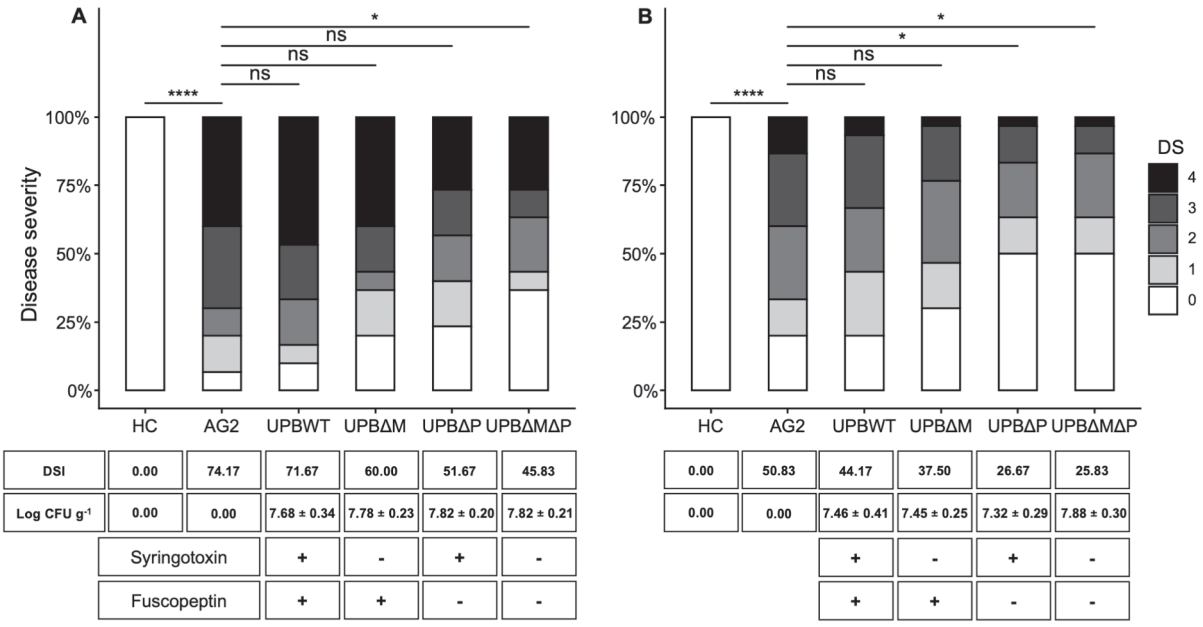

Fig. 7. Biocontrol of *R. solani* AG 2–2 by *P. fuscovaginae* UPB0736 and its CLP mutants in bean plants at 28 °C. Stacked bar charts show the percentage distribution of disease scales (DS0–DS4) for each treatment (n = 30 plants per treatment) across two independent experimental repeats (A and B). Disease severity index (DSI) and bacterial colonization (log CFU/g of root tissue) values are displayed below the plots for each treatment. Kruskal-Wallis tests showed significant differences among treatments in both experiments ($p < 0.0001$; Table S6). Significance levels above the plots represent pairwise Wilcoxon rank-sum tests with Benjamini–Hochberg correction comparing the positive disease control (AG 2–2) with all other treatments ($p \geq 0.05$ = ns; $0.01 \leq p < 0.05$ = * and $p < 0.0001$ = ****). No significant tray effects were observed in either repeat. HC represents the healthy control (non-inoculated plants).

The standard model confirmed that UPBWT provided no significant reduction in disease relative to pathogen control ($\beta = -0.088$, $p = 0.7850$). However, significant reductions were achieved by the fuscopeptin mutant UPBΔP ($p = 0.0011$) and the double mutant UPBΔMΔP ($p = 0.0002$). Tukey-adjusted comparisons confirmed that UPBΔP ($p = 0.0018$) and UPBΔMΔP ($p = 0.0096$) differed significantly from the pathogen control, while UPBWT did not ($p = 0.9988$). Also, the double mutant UPBΔMΔP provided significantly better protection than the wild-type ($p = 0.0046$).

A lower disease severity score was observed for UPBΔP and UPBΔMΔP, along with a better predicted probability of successful disease control (Health Probability) ranging from 42.2–62.2% to 46.4–66.2%, respectively, compared to 21.5–38.2% for UPBWT (Table S8C).

3.7. Global interaction of temperature and biocontrol

To systematically evaluate the relationship between temperature and biocontrol, a global cumulative link model was fitted to the entire dataset. A highly significant interaction between treatment and temperature was observed ($p < 0.001$), confirming that the biocontrol efficacy of UPB0736 and its mutants was highly temperature-dependent.

At 18 °C temperature, the UPBWT provided the strongest disease protection relative to the pathogen control ($p < 0.0001$), whereas the double mutant (UPBΔMΔP) showed no significant protective effect ($p = 0.9328$). This relationship, however, had a significant reversal at 28 °C. The positive significant interaction for UPBWT ($\beta = 1.285$; $p = 0.0055$) indicated decreased effectiveness at higher temperatures compared to UPBWT at 18 °C. In contrast, the double mutant showed a significant increase in efficacy at 28 °C, as indicated by a strong negative

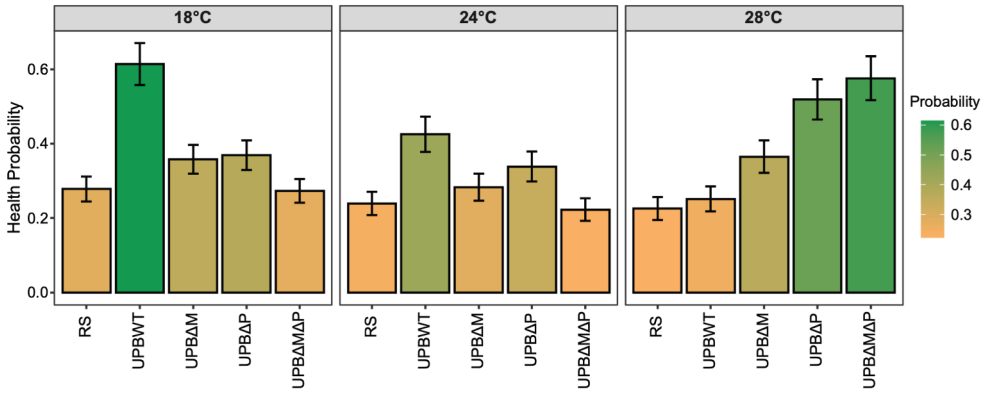

Fig. 8. Health probabilities for treatments across three temperatures: 18, 24, and 28 °C. Health Probability represents the probability of biocontrol success and is measured as the proportion of plants remaining in low-disease-severity classes (DS0–DS1). For the pathogen control (RS), Health Probability represents the baseline probability of low disease severity in the absence of biocontrol. Bars represent estimated probabilities from a cumulative link model, with error bars indicating standard errors (S.E.). Facets show different temperatures, and color intensity indicates the level of biocontrol success.

interaction ($\beta = -1.575$; $p = 0.0007$) (Table S10).

Predicted success probabilities derived from the global CLM, expressed as health probability, revealed a complete inversion of efficacy at the two temperature extremes. At 18 °C, the UPBWT exhibited a Health Probability of 61.4% compared to 27.3% for the double mutant. Conversely, at 28 °C, the UPBWT success dropped to 25.1%, while that of the double mutant (UPBΔMΔP) increased to 57.6% (Fig. 8; Table S11). This observation further confirmed the opposing nature: the UPB0736 wild-type is most effective at 18 °C, whereas CLP-deficient mutants provided better protection at 28 °C, demonstrating a pronounced temperature-dependent reversal.

4. Discussion

This study clearly demonstrates that the antifungal activity of *P. fuscovaginae* UPB0736 against *R. solani* depends on three major factors: temperature, the ability of UPB0736 to secrete CLPs, and the pathogen's anastomosis group. Importantly, UPB0736 and its CLP-deficient mutants were non-pathogenic toward common bean under all tested experimental conditions, as evidenced by the lack of symptoms in pathogen-free, bacteria-only treatments.

At 18 °C, UPB0736 wild-type effectively controlled the disease, and the effect was lost when both syringotoxin and fuscopeptin were absent. At 24 °C, the biocontrol effect of the wild-type was reduced, and no significant disease suppression was observed for any of the CLP mutants. At 28 °C, the wild-type showed no protective effect, whereas mutants lacking fuscopeptin or both CLPs showed significant disease suppression against AG 2–2. These findings highlight that CLPs and environmental factors, particularly temperature, play essential roles in the effectiveness and mechanisms of bacterial biocontrol agents.

4.1. *P. fuscovaginae UPB0736's biocontrol is CLP-mediated*

This study showed that a sufficient CLP level is essential for effective disease suppression. In the global CLM model, at low temperatures (18 °C), UPB0736 wild-type was highly effective, reaching 61.1–64.2% predicted health probability. This protection was strongly CLP-dependent, as the absence of syringotoxin and fuscopeptin reduced health probability to levels indistinguishable from the pathogen control (27%). Several past studies support the role of bacterial cyclic lipopeptides in suppressing fungal diseases. *Pseudomonas* strain CMR12a, which produces both phenazines and CLPs, effectively reduced *Rhizoctonia* root rot in beans, while mutants lacking both compound classes lost biocontrol (D'aes et al., 2011). According to Oni et al. (2022), bacteria belonging to the *Pseudomonas* taxa produce diverse CLPs that play a role in antagonism against fungal pathogens and in plant–microbe interactions.

P. fuscovaginae UPB0736, used in this study, produces two important metabolites, syringotoxin and fuscopeptin. These two CLPs, along with similar mycins and peptins produced by other *Pseudomonas* strains, are known for their antifungal activity (Zakharova et al., 2025; Zhou et al., 2024). The mechanisms and modes of action reported for these two CLPs include membrane permeability disruption (Bidwai et al., 1987), plasma membrane perturbations (Takemoto et al., 1989), and inhibition of plasma membrane H^+ − ATPase activity (Che et al., 1992).

4.2. *P. fuscovaginae UPB0736's biocontrol is temperature-dependent*

The temperature-dependent *in planta* antifungal activity of UPB0736 strongly aligns with earlier research by De Rop et al. (2025). They showed that *in vitro*, UPB0736 produces the highest levels of syringotoxin and fuscopeptin at 18 °C, with levels decreasing sharply at 28 °C. The reduction in syringotoxin with increasing temperature was more pronounced than that observed for fuscopeptin. Importantly, *in vitro* antagonistic assays with UPB0736 supernatant at 18 °C and 28 °C revealed potent antifungal activity across both temperatures against both *R. solani* anastomosis groups. De Rop et al. (2025) previously showed that the sensitivity of *R. solani* to specialized metabolites in the UPB0736 supernatant is primarily due to syringotoxin. IC_{50} determinations based on purified syringotoxin yielded the same results as IC_{50} determinations based on the supernatant of the UPB0736 wild-type strain, in which the concentration of syringotoxin was chemically analyzed. The use of UPB0736 supernatant in our work shows that *R. solani* AG 5 is less sensitive to syringotoxin (deduced IC_{50}: 0.11–0.14 mg/L) than *R. solani* AG 2–2 (IC_{50}: 0.08–0.09 mg/L) (Table S5), which is also apparent from the *in vitro* dual culture assays (Fig. 4). Collectively, these findings suggest that reduced biocontrol efficacy at higher temperatures is not due to reduced sensitivity of the fungus, but rather due to low CLP production levels.

Therefore, effective biocontrol may depend on achieving sufficient CLP accumulation in the plant, which probably occurs only at low temperatures. Temperature-dependent modulation of biocontrol factor production has been observed in previous research. In *P. protegens* CHA0, expression of antibiotics and hydrogen cyanide was lower at 35 °C than at 30 °C. This temperature-dependent regulation has been linked to the sensor kinase RetS, which functions as a thermal integrator by modulating the Gac/Rsm signal transduction pathway at high temperature (Humair et al., 2009). Shanahan et al. (1992) demonstrated that in *Pseudomonas* sp. strain F113 (now classified as *P. ogarae* F113), production of the antifungal compound 2,4-diacetyl phloroglucinol was maximum at 12 °C. Similarly, in *P. fluorescens* In5, production of the nunamycin and nunapeptin CLPs was optimal at low temperatures (10–15 °C) and strongly reduced at higher temperatures (~28 °C) (Christiansen et al., 2020). Production of the CLP putisolvin in *P. putida* PCL1445 is also upregulated at low temperature, and requires the heat shock proteins DnaK and DnaJ. These heat shock proteins may be required for proper folding or activity of transcriptional factors or for assembly of non-ribosomal peptide synthetase complexes responsible for synthesizing CLPs (Dubern et al., 2005). Investigating similar regulatory networks in *P. fuscovaginae* UPB0736 will be of significant interest for improving our understanding of temperature-responsive environmental sensing in this strain.

Temperature-dependent *in planta* biocontrol has been observed in other beneficial bacteria (Landa et al., 2001; Wei et al., 2017), but was attributed to fluctuations in root colonization density or competitive growth dynamics. To our knowledge, this is the first report describing temperature-dependent biocontrol in which efficacy is governed by the regulation of bioactive metabolites rather than bacterial population dynamics.

4.3. *Inconsistency in biocontrol at 24 °C*

In four separate plant bioassays conducted at 24 °C against *R. solani* AG 2–2, UPB0736 reduced disease severity, but the effect was inconsistent across assays (Fig. 2). While individual experiments showed alternating significant and non-significant results, ordinal regression analysis indicated an overall reduction in disease severity, with a 64% decrease in the odds of plants reaching higher disease-severity categories. Partial proportional odds modeling further revealed that UPB0736 had its strongest effect at the lowest disease threshold (DS0–DS1), with diminishing impact at higher severity levels.

These observations suggest that UPB0736 primarily acts as a protective agent, delaying early disease development rather than reversing advanced symptoms. This threshold-dependent protection aligns with reduced but still present CLP production at 24 °C, where antifungal concentrations may be enough to limit initial pathogen invasion but insufficient to suppress fully established infections. These CLP levels may moderately restrict pathogen growth, allowing some *Rhizoctonia* mycelium to persist in the rhizosphere and occasionally establish infection, resulting in moderate-to-high disease levels.

4.4. Loss of UPB0736 wild-type biocontrol activity at 28 °C

CLPs contribute to biocontrol at 18 °C and 24 °C, whereas at 28 °C, biocontrol is observed only in the absence of both syringotoxin and fuscopeptin. This unexpected increase in biocontrol in UPB0736 CLP mutants at 28 °C, but not at 18 °C or in the wild-type at either temperature, is particularly noteworthy.

We hypothesize that this phenomenon is driven by a complex interplay between the different metabolites produced by UPB0736 and the plant's hormonal signaling pathways. At 28 °C, in the absence of the antifungal CLPs (syringotoxin and fuscopeptin), the third CLP, asplenin, may act as a signaling molecule to trigger Induced Systemic Resistance (ISR). Asplenin is probably only active at triggering ISR at low concentrations. It has been shown before that CLPs orfamide and sessilin originating from *Pseudomonas sessilinigenes* CMR12a induce ISR against web blight in bean plants caused by *R. solani* AG 2–2. This ISR was observed at concentrations of 1–100 nM for orfamide and 0.5–5 nM for sessilin, whereas higher concentrations of these metabolites were inactive (Ma et al., 2016). De Rop et al. (2025) showed that *in vitro* asplenin production in UPB0736 is lower at 28 °C than at 18 °C. We are currently investigating whether low concentrations of asplenin can prime plant defense against *R. solani*.

We propose that this ISR activity of asplenin is masked by the presence of syringotoxin and fuscopeptin at 28 °C in the wild-type strain UPB0736. Low concentrations of syringotoxin and fuscopeptin at 28 °C may increase plant susceptibility to *R. solani*. Syringotoxin in rice plasma membranes *in vitro* stimulated H^+ − ATPase activity at low concentrations (<80 μM) but inhibited it at higher concentrations (>160 μM) (Batoko et al., 1998). Fuscopeptin, although it consistently inhibited plant plasma membrane H^+ − ATPase activity at all concentrations, formed small, transient ion-conducting pores at low concentrations (3–40 nM), but created larger, membrane-disrupting pores at high concentrations (≥40 nM) (Batoko et al., 1998; Coraiola et al., 2008).

Although the effect of these CLPs at low concentrations on H^+−ATPase activity appears distinct, the upregulation of plasma membrane H^+−ATPase is correlated with shifts in defense gene expression patterns typically associated with SA-mediated responses (Schaller and Oecking, 1999; Yuan et al., 2009; Falhof et al., 2016). Fuscopeptin-induced sublethal pores can cause ion imbalances and rapid Ca^{2+} influx, which serve as early signals in plant immune signaling (Köster et al., 2022) and subsequently trigger events that may modulate downstream SA-associated pathways (Schaller and Oecking, 1999; Seybold et al., 2014).

SA-associated signaling can antagonistically suppress JA-dependent defenses (Pieterse et al., 2012; Spoel et al., 2007; Van der Does et al., 2013). This hormonal cross-talk can potentially increase susceptibility to necrotrophic pathogens, such as *R. solani*, which are primarily controlled by JA-mediated pathways (Glazebrook, 2005; Govrin and Levine, 2000). Effectors of *R. solani* have been reported to interfere with host hormone signaling, promoting susceptibility by suppressing JA-dependent defenses (Wang et al., 2025).

At 18 °C, bean plant health is determined by the direct antifungal activity of the CLPs, and potential effects on plant defense are likely overridden at high CLP concentrations. At 28 °C, however, we cannot rule out the production and involvement of other metabolites besides CLPs, including volatile compounds and siderophores (Bailly and Weisskopf, 2017; Haas and Défago, 2005; Loper et al., 2012; Pieterse et al., 2014; Garbeva and Weisskopf, 2020; Raio, 2024). Furthermore, as observed in *P. protegens* Pf-5, the disruption of a metabolite biosynthetic pathway can trigger pleiotropic effects that redirect metabolic flux toward other secondary metabolites (Quecine et al., 2016). A similar metabolic redirection in UPB0736 could contribute to the CLP-independent protection observed at 28 °C, although comprehensive metabolomic profiling will be required to verify whether such compensatory mechanisms exist. Finally, a major limitation in fully validating these concentration-dependent hypotheses is the technical difficulty of directly quantifying the *in situ* CLP concentrations within the rhizosphere, an area that remains a critical focus for future analytical investigation.

4.5. Colonization by P. fuscovaginae UPB0736

The effectiveness of biocontrol in UPB0736 is primarily determined by CLP production rather than root colonization. UPB0736 and its CLP-deficient mutants consistently colonized bean roots across all tested temperatures. This suggests that the observed variation in biocontrol efficiency across different temperatures was not due to differences in colonization. This contrasts with previous studies that link reduced biocontrol efficiency to poor colonization at elevated temperatures (Wei et al., 2017).

But the finding aligns with Schmidt et al. (2004), who reported that the population density of *P. fluorescens* B5 on sugar beet roots remained consistent across soil temperatures ranging from 5 to 25 °C. Similarly, Seong et al. (1991) demonstrated that *P. fluorescens* ANP15 and *P. aeruginosa* 7NSK2 maintained similar maize root occupancy across a broad temperature range of 18–30 °C.

The loss of CLPs can affect bacterial population dynamics as *P. fluorescens* SBW25 mutants lacking the CLP viscosin showed reduced root colonization in the wheat rhizosphere (Guan et al., 2024). However, the UPB0736 CLPs knockout mutants used in this study, which lack syringotoxin and fuscopeptin, did not affect root colonization. These CLPs contribute to microbial competition, virulence factors for phytotoxicity, and nutrient release from the surrounding host (Bender et al., 1999; Bigirimana et al., 2015; Ferrarini et al., 2022; Geudens and Martins, 2018), but they do not directly affect bacterial motility or root colonization.

5. Conclusion

The biocontrol activity of *P. fuscovaginae* UPB0736 against *R. solani* is not governed by a single mechanism but rather by a complex, dynamic interplay among factors such as temperature, CLP production, and the pathogen. The activity is mainly driven by CLPs. Disease suppression by the wild-type strain is most potent at 18 °C, weakened and inconsistent at 24 °C, and completely lost at 28 °C. Interestingly, at 28 °C, a reversal in the functional activity of CLP was observed, as CLP-deficient mutants gained biocontrol activity, whereas the wild-type lost it.

This study offers several novel insights. It is the first report of metabolite-mediated temperature-dependent biocontrol *in planta* and shows that variation in biocontrol efficacy with temperature is attributable to regulation of the CLPs (syringotoxin and fuscopeptin) rather than to fluctuations in root colonization. Moreover, a unique enhancement in biocontrol activity by CLP-deficient mutants was observed at 28 °C, compared with the wild-type. These findings emphasize the complexity of *Pseudomonas*-mediated biocontrol and exemplify why translating *in vitro*-observed biocontrol to real-world applications is often challenging and unsuccessful.

The molecular mechanisms underlying temperature-dependent variation in CLP production and biocontrol remain to be further studied. We are currently investigating the role of asplenin and the involvement of plant immune signaling in the observed biocontrol at 28 °C in the absence of syringotoxin and fuscopeptin. Overall, future studies should prioritize interactions among CLPs, plant immune responses, pathogen virulence, and environmental factors to better understand context-dependent biocontrol outcomes.

CRediT authorship contribution statement

Bishnu Prasad Marahatta: Writing – original draft, Visualization, Methodology, Investigation, Funding acquisition, Formal analysis, Data curation, Conceptualization. **Monica Höfte:** Writing – review & editing, Supervision, Resources, Project administration, Funding acquisition,

Conceptualization.

Declaration of competing interest

The authors declare that they have no known competing financial interests or personal relationships that could have influenced the work reported in this paper.

Acknowledgements

B. Marahatta is a doctoral fellow funded by the Research Foundation - Flanders, Belgium (FWO) through a PhD fellowship in Strategic Basic Research (SB) [FWO ID: 1S93425N]. The authors thank Dr. Lu Zhou for critically reading the manuscript and also wish to extend their gratitude to all technicians and colleagues at the Phytopathology Laboratory, Department of Plants and Crops, Ghent University.

Appendix A. Supplementary data

Supplementary data to this article can be found online at https://doi.org/10.1016/j.biocontrol.2026.106073. Supplementary data consist of 8 tables with statistical details of all experiments.

References

Ajayi-Oyetunde, O.O., Bradley, C.A., 2018. *Rhizoctonia solani*: taxonomy, population biology and management of *Rhizoctonia* seedling disease of soybean. Plant Pathol. 67, 3–17. https://doi.org/10.1111/ppa.12733.

Akber, M.A., Mubeen, M., Sohail, M.A., Khan, S.W., Solanki, M.K., Khalid, R., Abbas, A., Divvela, P.K., Zhou, L., 2023. Global distribution, traditional and modern detection, diagnostic, and management approaches of *Rhizoctonia solani* associated with legume crops. Front. Microbiol. 13, 1091288. https://doi.org/10.3389/fmicb.2022.1091288.

Bailly, A., Weisskopf, L., 2017. Mining the volatilomes of plant-associated microbiota for new biocontrol solutions. Front. Microbiol. 8, 1638. https://doi.org/10.3389/fmicb.2017.01638.

Ballio, A., Bossa, F., Camoni, L., Di Giorgio, D., Flamand, M.C., Maraite, H., Nitti, G., Pucci, P., Scaloni, A., 1996. Structure of fuscopeptins, phytotoxic metabolites of *Pseudomonas fuscovaginae*. FEBS Lett. 381, 213–216. https://doi.org/10.1016/0014-5793(96)00043-9.

Ballio, A., Bossa, F., Collina, A., Gallo, M., Iacobellis, N.S., Paci, M., Pucci, P., Scaloni, A., Segre, A., Simmaco, M., 1990. Structure of syringotoxin, a bioactive metabolite of *Pseudomonas syringae* pv. *syringae*. FEBS Lett. 269, 377–380. https://doi.org/10.1016/0014-5793(90)81197-V.

Batoko, H., De Kerchove D'Exaerde, A., Kinet, J.M., Bouharmont, J., Gage, R.A., Maraite, H., Boutry, M., 1998. Modulation of plant plasma membrane H^+-ATPase by phytotoxic lipodepsipeptides produced by the plant pathogen *Pseudomonas fuscovaginae*. Biochim. Biophys. Acta Biomembr. 1372, 216–226. https://doi.org/10.1016/S0005-2736(98)00060-1.

Bender, C.L., Alarcón-Chaidez, F., Gross, D.C., 1999. *Pseudomonas syringae* phytotoxins: mode of action, regulation, and biosynthesis by peptide and polyketide synthetases. Microbiol. Mol. Biol. Rev. 63, 266–292. https://doi.org/10.1128/MMBR.63.2.266-292.1999.

Bender, C.L., Scholz-Schroeder, B.K., 2004. New insights into the biosynthesis, mode of action, and regulation of syringomycin, syringopeptin, and coronatine. In: Ramos, J.-L. (Ed.), *Pseudomonas*: Volume 2: Virulence and Gene Regulation. Springer, New York, pp. 125–158. https://doi.org/10.1007/978-1-4419-9084-6_4.

Bhuiyan, M.Z.R., Mendoza, L.D.R., Lakshman, D.K., Qi, A., Khan, M., 2025. Effects of inoculum density of *R. solani* AG 2-2IIIB and age of plant on root rot severity in sugar beet. J. Plant Prot. Res. 65, 125–132. https://doi.org/10.24425/jppr.2025.153824.

Bidwai, A.P., Zhang, L., Bachmann, R.C., Takemoto, J.Y., 1987. Mechanism of action of *Pseudomonas syringae* phytotoxin, syringomycin. Plant Physiol. 83, 39–43. https://doi.org/10.1104/pp.83.1.39.

Bigirimana, V.de P., Hua, G.K.H., Nyamangyoku, O.I., Höfte, M., 2015. Rice sheath rot: an emerging ubiquitous destructive disease complex. Front. Plant Sci. 6, 1066. https://doi.org/10.3389/fpls.2015.01066.

Bolkan, H.A., 1985. Anastomosis groups and pathogenicity of *Rhizoctonia solani* isolates from Brazil. Plant Dis. 69, 599. https://doi.org/10.1094/pd-69-599.

Canpolat, S., Woodward, S., Kurbetli, İ., 2023. Molecular and pathological characterization of the isolates of *Rhizoctonia* spp. associated with dry bean (*Phaseolus vulgaris*) in Türkiye. J. Plant Pathol. 105, 837–848. https://doi.org/10.1007/s42161-023-01377-2.

Carling, D.E., 1996. Grouping in *Rhizoctonia solani* by hyphal anastomosis reaction. In: Sneh, B., Jabaji-Hare, S., Neate, S., Dijst, G. (Eds.), *Rhizoctonia* Species: Taxonomy, Molecular Biology, Ecology, Pathology and Disease Control. Springer, Netherlands, Dordrecht, pp. 37–47. https://doi.org/10.1007/978-94-017-2901-7_3.

Che, F., Kasamo, K., Fukuchi, N., Isogai, A., Suzuki, A., 1992. Bacterial phytotoxins, syringomycin, syringostatin and syringotoxin, exert their effect on the plasma membrane H^+-ATPase partly by a detergent-like action and partly by inhibition of the enzyme. Physiol. Plant. 86, 518–524. https://doi.org/10.1111/j.1399-3054.1992.tb02164.x.

Christiansen, L., Alanin, K.S., Phippen, C.B.W., Olsson, S., Stougaard, P., Hennessy, R.C., 2020. Fungal-associated molecules induce key genes involved in the biosynthesis of the antifungal secondary metabolites nunamycin and nunapeptin in the biocontrol strain *Pseudomonas fluorescens* In5. Appl. Environ. Microbiol. 86, e01284–e01320. https://doi.org/10.1128/AEM.01284-20.

Coraiola, M., Paletti, R., Fiore, A., Fogliano, V., Serra, M.D., 2008. Fuscopeptins, antimicrobial lipodepsipeptides from *Pseudomonas fuscovaginae*, are channel forming peptides active on biological and model membranes. J. Pept. Sci. 14, 496–502. https://doi.org/10.1002/psc.970.

Cubeta, M.A., Vilgalys, R., 1997. Population biology of the *Rhizoctonia solani* complex. Phytopathology 87, 480–484. https://doi.org/10.1094/PHYTO.1997.87.4.480.

D'aes, J., Hua, G.K.H., De Maeyer, K., Pannecoucque, J., Forrez, I., Ongena, M., Dietrich, L.E.P., Thomashow, L.S., Mavrodi, D.V., Höfte, M., 2011. Biological control of *Rhizoctonia* root rot on bean by phenazine- and cyclic Lipopeptide-producing *Pseudomonas* CMR12a. Phytopathology 101, 996–1004. https://doi.org/10.1094/PHYTO-11-10-0315.

De Rop, J., Prasad, D., Geudens, N., Zhou, L., Marahatta, B., Spanoghe, P., Martins, J.C., Höfte, M., 2025. Temperature-dependent production of cyclic lipopeptides by *Pseudomonas fuscovaginae* UPB0736 and its impact on *Rhizoctonia solani* suppression. The Microbe 8, 100530. https://doi.org/10.1016/j.microb.2025.100530.

Dubern, J., Lagendijk, E.L., Lugtenberg, B.J.J., Bloemberg, G.V., 2005. The heat shock genes *dnaK*, *dnaJ*, and *grpE* are involved in regulation of putisolvin biosynthesis in *Pseudomonas putida* pcl1445. J. Bacteriol. 187, 5967–5976. https://doi.org/10.1128/jb.187.17.5967-5976.2005.

Duveiller, E., Notteghem, J.L., Rott, P., Snacken, F., Maraite, H., 1990. Bacterial sheath brown rot of rice caused by *Pseudomonas fuscovaginae* in Malagasy. Trop. Pest Manag. 36, 151–153. https://doi.org/10.1080/09670879009371461.

Eken, C., Demirci, E., 2004. Anastomosis groups and pathogenicity of *Rhizoctonia solani* and binucleate *Rhizoctonia* isolates from bean in Erzurum, Turkey. J. Plant Pathol. 86, 49–52.

Falhof, J., Pedersen, J.T., Fuglsang, A.T., Palmgren, M., 2016. Plasma membrane H^+-ATPase regulation in the center of plant physiology. Mol. Plant 9, 323–337. https://doi.org/10.1016/j.molp.2015.11.002.

Ferrarini, E., Špacapan, M., Lam, V.B., McCann, A., Cesa-Luna, C., Marahatta, B.P., De Pauw, E., De Mot, R., Venturi, V., Höfte, M., 2022. Versatile role of *Pseudomonas fuscovaginae* cyclic lipopeptides in plant and microbial interactions. Front. Plant Sci. 13, 1008980. https://doi.org/10.3389/fpls.2022.1008980.

Garbeva, P., Weisskopf, L., 2020. Airborne signals: Volatile communication between plants and microbes. New Phytol. 226, 32–43. https://doi.org/10.1111/nph.16282.

Geudens, N., Martins, J.C., 2018. Cyclic lipodepsipeptides from *Pseudomonas* spp. - biological swiss-army knives. Front. Microbiol. 9, 1867. https://doi.org/10.3389/fmicb.2018.01867.

Girard, L., Höfte, M., De Mot, R., 2020. Lipopeptide families at the interface between pathogenic and beneficial *Pseudomonas*-plant interactions. Crit. Rev. Microbiol. 46, 397–419. https://doi.org/10.1080/1040841X.2020.1794790.

Girard, L., Lood, C., Höfte, M., Vandamme, P., Rokni-Zadeh, H., Van Noort, V., Lavigne, R., De Mot, R., 2021. The ever-expanding *Pseudomonas* genus: description of 43 new species and partition of the *Pseudomonas putida* group. Microorganisms 9, 1766. https://doi.org/10.3390/microorganisms9081766.

Glazebrook, J., 2005. Contrasting mechanisms of defense against biotrophic and necrotrophic pathogens. Annu. Rev. Phytopathol. 43, 205–227. https://doi.org/10.1146/annurev.phyto.43.040204.135923.

Godoy-Lutz, G., Kuninaga, S., Steadman, J.R., Powers, K., 2008. Phylogenetic analysis of *Rhizoctonia solani* subgroups associated with web blight symptoms on common bean based on ITS-5.8S rDNA. J. Gen. Plant Pathol. 74, 32–40. https://doi.org/10.1007/s10327-007-0060-6.

González García, V., Portal Onco, M.A., Rubio Susan, V., 2006. Review. Biology and systematics of the form genus *Rhizoctonia*. Span. J. Agric. Res. 4, 55–79. https://doi.org/10.5424/sjar/2006041-178.

Götze, S., Stallforth, P., 2020. Structure, properties, and biological functions of nonribosomal lipopeptides from *Pseudomonads*. Nat. Prod. Rep. 37, 29–54. https://doi.org/10.1039/c9np00022d.

Govrin, E.M., Levine, A., 2000. The hypersensitive response facilitates plant infection by the necrotrophic pathogen *Botrytis cinerea*. Curr. Biol. 10, 751–757. https://doi.org/10.1016/S0960-9822(00)00560-1.

Guan, Y., Bak, F., Hennessy, R.C., Horn Herms, C., Elberg, C.L., Dresbøll, D.B., Winding, A., Sapkota, R., Nicolaisen, M.H., 2024. The potential of Pseudomonas fluorescens SBW25 to produce viscosin enhances wheat root colonization and shapes root-associated microbial communities in a plant genotype-dependent manner in soil systems. mSphere 9, e00294–e00324. https://doi.org/10.1128/msphere.00294-24.

Haas, D., Défago, G., 2005. Biological control of soil-borne pathogens by fluorescent *Pseudomonads*. Nat. Rev. Microbiol. 3, 307–319. https://doi.org/10.1038/nrmicro1129.

Hesse, C., Schulz, F., Bull, C.T., Shaffer, B.T., Yan, Q., Shapiro, N., Hassan, K.A., Varghese, N., Elbourne, L.D.H., Paulsen, I.T., Kyrpides, N., Woyke, T., Loper, J.E., 2018. Genome-based evolutionary history of *Pseudomonas* spp. Environ. Microbiol. 20, 2142–2159. https://doi.org/10.1111/1462-2920.14130.

Höfte, M., 2021. The use of *Pseudomonas* spp. as bacterial biocontrol agents to control plant disease. In: Köhl, J., Ravensberg, W.J. (Eds.), Microbial Bioprotectants for Plant Disease Management. Burleigh Dodds Science Publishing, Cambridge, UK, pp. 301–374 https://doi.org/10.19103/AS.2021.0093.11.

Humair, B., González, N., Mossialos, D., Reimmann, C., Haas, D., 2009. Temperature-responsive sensing regulates biocontrol factor expression in *Pseudomonas fluorescens* CHA0. ISME J. 3, 955–965. https://doi.org/10.1038/ismej.2009.42.

Köster, P., DeFalco, T.A., Zipfel, C., 2022. Ca^{2+} signals in plant immunity. EMBO J. 41. https://doi.org/10.15252/embj.2022110741.

Kovács, B., Prasad, D., De Roo, V., Vanheede, M., Muangkaew, P., Madder, A., Höfte, M., De Mot, R., Geudens, N., Martins, J.C., 2025. Higher-level structural classification of *Pseudomonas* cyclic lipopeptides through their bioactive conformation. Adv. Sci. 13, e20365. https://doi.org/10.1002/advs.202520365.

Landa, B.B., Navas-Cortés, J.A., Hervás, A., Jiménez-Díaz, R.M., 2001. Influence of temperature and inoculum density of Fusarium oxysporum f. sp. ciceris on suppression of *Fusarium* wilt of chickpea by rhizosphere bacteria. Phytopathology 91, 807–816. https://doi.org/10.1094/PHYTO.2001.91.8.807.

Lavermicocca, P., Sante Iacobellis, N., Simmaco, M., Graniti, A., 1997. Biological properties and spectrum of activity of *Pseudomonas syringae* pv. *syringae* toxins. Physiol. Mol. Plant Pathol. 50, 129–140. https://doi.org/10.1006/pmpp.1996.0078.

Loper, J.E., Hassan, K.A., Mavrodi, D.V., Davis II, E.W., Lim, C.K., Shaffer, B.T., Elbourne, L.D.H., Stockwell, V.O., Hartney, S.L., Breakwell, K., Henkels, M.D., Tetu, S.G., Rangel, L.I., Kidarsa, T.A., Wilson, N.L., van de Mortel, J.E., Song, C., Blumhagen, R., Radune, D., Hostetler, J.B., Brinkac, L.M., Durkin, A.S., Kluepfel, D. A., Wechter, W.P., Anderson, A.J., Kim, Y.C., Pierson III, L.S., Pierson, E.A., Lindow, S.E., Kobayashi, D.Y., Raaijmakers, J.M., Weller, D.M., Paulsen, I.T., 2012. Comparative genomics of plant-associated *Pseudomonas* spp.: Insights into diversity and inheritance of traits involved in multitrophic interactions. PLoS Genet. 8, e1002784. https://doi.org/10.1371/journal.pgen.1002784.

Ma, Z., Hua, G.K.H., Ongena, M., Höfte, M., 2016. Role of phenazines and cyclic lipopeptides produced by *Pseudomonas* sp. CMR12a in induced systemic resistance on rice and bean. Environ. Microbiol. Rep. 8, 896–904. https://doi.org/10.1111/1758-2229.12454.

Malfanova, N., Franzil, L., Lugtenberg, B., Chebotar, V., Ongena, M., 2012. Cyclic lipopeptide profile of the plant-beneficial endophytic bacterium *Bacillus subtilis* HC8. Arch. Microbiol. 194, 893–899. https://doi.org/10.1007/s00203-012-0823-0.

Marcou, S., Wikström, M., Ragnarsson, S., Persson, L., Höfte, M., 2021. Occurrence and anastomosis grouping of *Rhizoctonia* spp. inducing black scurf and greyish-white felt-like mycelium on carrot in Sweden. J. Fungi 7, 396. https://doi.org/10.3390/jof7050396.

Miyajima, K., Tanii, A., Akita, T., 1983. *Pseudomonas fuscovaginae* sp. nov., nom. rev. Int. J. Syst. Evol. Microbiol. 33, 656–657. https://doi.org/10.1099/00207713-33-3-656.

Nandeesha, C.V., Nandeesha, K.L., Bhaliya, C.M., 2021. Evolutionary biology and interaction among the anastomosis groups of *Rhizoctonia* spp. J. Pharmacogn. Phytochem. 10, 461–466. https://doi.org/10.22271/phyto.2021.v10.i2f.13840.

Nerey, Y., Pannecoucque, J., Hernandez, H.P., Diaz, M., Espinosa, R., De Vos, S., Van Beneden, S., Herrera, L., Höfte, M., 2010. *Rhizoctonia* spp. causing root and hypocotyl rot in *Phaseolus vulgaris* in Cuba. J. Phytopathol. 158, 236–243. https://doi.org/10.1111/j.1439-0434.2009.01609.x.

Nybroe, O., Sørensen, J., 2004. Production of cyclic lipopeptides by fluorescent *Pseudomonads*, in: Ramos, J.L. (Eds.), *Pseudomonas*. Springer, Boston, MA, 147–172. https://doi.org/10.1007/978-1-4419-9088-4_5.

Oni, F.E., Esmaeel, Q., Onyeka, J.T., Adeleke, R., Jacquard, C., Clement, C., Gross, H., Ait Barka, E., Höfte, M., 2022. *Pseudomonas* lipopeptide-mediated biocontrol: chemotaxonomy and biological activity. Molecules 27, 372. https://doi.org/10.3390/molecules27020372.

Patel, H.K., da Silva, D.P., Devescovi, G., Maraite, H., Paszkiewicz, K., Studholme, D.J., Venturi, V., 2012. Draft genome sequence of *Pseudomonas fuscovaginae*, a broad-host-range pathogen of plants. J. Bacteriol. 194, 2765–2766. https://doi.org/10.1128/JB.00341-12.

Pieterse, C.M.J., Zamioudis, C., Berendsen, R.L., Weller, D.M., Van Wees, S.C.M., Bakker, P.A.H.M., 2014. Induced systemic resistance by beneficial microbes. Annu. Rev. Phytopathol. 52, 347–375. https://doi.org/10.1146/annurev-phyto-082712-102340.

Pieterse, C.M.J., Van der Does, D., Zamioudis, C., Leon-Reyes, A., Van Wees, S.C.M., 2012. Hormonal modulation of plant immunity. Annu. Rev. Cell Dev. Biol. 28, 489–521. https://doi.org/10.1146/annurev-cellbio-092910-154055.

Quecine, M.C., Kidarsa, T.A., Goebel, N.C., Shaffer, B.T., Henkels, M.D., Zabriskie, T.M., Loper, J.E., 2016. An interspecies signaling system mediated by fusaric acid has parallel effects on antifungal metabolite production by *Pseudomonas protegens* strain pf-5 and antibiosis of *Fusarium* spp. Appl. Environ. Microbiol. 82, 1372–1382. https://doi.org/10.1128/AEM.02574-15.

Raaijmakers, J.M., de Bruijn, I., de Kock, M.J.D., 2006. Cyclic lipopeptide production by plant-associated *Pseudomonas* spp.: diversity, activity, biosynthesis, and regulation. Mol. Plant Microbe Interact. 19, 699–710. https://doi.org/10.1094/MPMI-19-0699.

Raaijmakers, J.M., de Bruijn, I., Nybroe, O., Ongena, M., 2010. Natural functions of lipopeptides from *Bacillus* and *Pseudomonas*: more than surfactants and antibiotics. FEMS Microbiol. Rev. 34, 1037–1062. https://doi.org/10.1111/j.1574-6976.2010.00221.x.

Raio, A., 2024. Diverse roles played by "*Pseudomonas fluorescens* complex" volatile compounds in their interaction with phytopathogenic microorganisms, pests and plants. World J. Microbiol. Biotechnol. 40, 80. https://doi.org/10.1007/s11274-023-03873-0.

Schaller, A., Oecking, C., 1999. Modulation of plasma membrane H^+-ATPase activity differentially activates wound and pathogen defense responses in tomato plants. Plant Cell 11, 263–272. https://doi.org/10.1105/tpc.11.2.263.

Schmidt, C.S., Agostini, F., Leifert, C., Killham, K., Mullins, C.E., 2004. Influence of soil temperature and matric potential on sugar beet seedling colonization and suppression of Pythium damping-off by the antagonistic bacteria *Pseudomonas fluorescens* and *Bacillus subtilis*. Phytopathology 94, 351–363. https://doi.org/10.1094/PHYTO.2004.94.4.351.

Seong, K.-Y., Höfte, M., Boelens, J., Verstraete, W., 1991. Growth, survival, and root colonization of plant growth beneficial *Pseudomonas fluorescens* ANP15 and *Pseudomonas aeruginosa* 7NSK2 at different temperatures. Soil Biol. Biochem. 23, 423–428. https://doi.org/10.1016/0038-0717(91)90004-4.

Seybold, H., Trempel, F., Ranf, S., Scheel, D., Romeis, T., Lee, J., 2014. Ca^{2+} signalling in plant immune response: from pattern recognition receptors to Ca^{2+} decoding mechanisms. New Phytol. 204, 782–790. https://doi.org/10.1111/nph.13031.

Shanahan, P., O'sullivan, D.J., Simpson, P., Glennon, J.D., O'Gara, F., 1992. Isolation of 2,4-diacetylphloroglucinol from a fluorescent pseudomonad and investigation of physiological parameters influencing its production. Appl. Environ. Microbiol. 58, 353–358. https://doi.org/10.1128/aem.58.1.353-358.1992.

Spoel, S.H., Johnson, J.S., Dong, X., 2007. Regulation of tradeoffs between plant defenses against pathogens with different lifestyles. PNAS 104, 18842–18847. https://doi.org/10.1073/pnas.0708139104.

Sun, M., Wang, H., Ye, G., Zhang, S., Li, Z., Cai, L., Wang, F., 2024. Biological characteristics and metabolic phenotypes of different anastomosis groups of *Rhizoctonia solani* strains. BMC Microbiol. 24, 217. https://doi.org/10.1186/s12866-024-03363-9.

Takemoto, J.Y., Giannini, J.L., Vassey, T., Briskin, D.P., 1989. Syringomycin effects on plasma membrane Ca+2 transport. In: Graniti, A., Durbin, R.D., Ballio, A. (Eds.), Phytotoxins and Plant Pathogenesis. Springer Berlin Heidelberg, Berlin, Heidelberg, pp. 167–175. https://doi.org/10.1007/978-3-642-73178-5_15.

Tanii, A., Miyajima, K., Akita, T., 1976. The sheath brown rot disease of rice plant and its causal bacterium, *Pseudomonas fuscovaginae* A. Tanii, K. Miyajima et T. Akita sp. nov. Ann. Phytopathol. Soc. Jpn. 42, 540–548. https://doi.org/10.3186/jjphytopath.42.540.

Tohya, M., Watanabe, S., Tada, T., Tin, H.H., Kirikae, T., 2020. Genome analysis-based reclassification of *Pseudomonas fuscovaginae* and *Pseudomonas shirazica* as later heterotypic synonyms of *Pseudomonas asplenii* and *Pseudomonas asiatica*, respectively. Int. J. Syst. Evol. Microbiol. 70, 3547–3552. https://doi.org/10.1099/ijsem.0.004199.

Valentín Torres, S., Vargas, M.M., Godoy-Lutz, G., Porch, T.G., Beaver, J.S., 2016. Isolates of *Rhizoctonia solani* can produce both web blight and root rot symptoms in common bean (*Phaseolus vulgaris* L.). Plant Dis. 100, 1351–1357. https://doi.org/10.1094/PDIS-11-15-1270-RE.

Van der Does, D., Leon-Reyes, A., Koornneef, A., Van Verk, M.C., Rodenburg, N., Pauwels, L., Goossens, A., Körbes, A.P., Memelink, J., Ritsema, T., Van Wees, S.C.M., Pieterse, C.M.J., 2013. Salicylic acid suppresses jasmonic acid signaling downstream of SCFCOI1-JAZ by targeting GCC promoter motifs via transcription factor ORA59. Plant Cell 25, 744–761. https://doi.org/10.1105/tpc.112.108548.

Wang, J., Zhang, J.X., Dai, X.F., Guo, Q.T., Chen, J.Y., Li, Y., Zhang, D.D., 2025. *Rhizoctonia solani* secretes RsCAP3 to target Nb14-3-3b, interfering with hormone-mediated resistance in *Nicotiana benthamiana*. J. Agric. Food Chem. 73, 16109–16120. https://doi.org/10.1021/acs.jafc.5c00921.

Weeraratne, K.N., 2018. Host preferences and pathogenomics of *Pseudomonas fuscovaginae* in Australia. Charles Sturt University, Australia. PhD thesis.

Weeraratne, N., Stodart, B.J., Venturi, V., Höfte, M., Hua, G.K.H., Ongena, M., Savocchia, S., Steel, C.C., Ash, G.J., 2020. Syringopeptin contributes to the virulence of *Pseudomonas fuscovaginae*, based on sypA biosynthesis mutant analysis. Phytopathology 110, 780–789. https://doi.org/10.1094/PHYTO-07-19-0235-R.

Wei, Z., Huang, J., Yang, T., Jousset, A., Xu, Y., Shen, Q., Friman, V.P., 2017. Seasonal variation in the biocontrol efficiency of bacterial wilt is driven by temperature-mediated changes in bacterial competitive interactions. J. Appl. Ecol. 54, 1440–1448. https://doi.org/10.1111/1365-2664.12873.

Yang, Q., Yang, L., Wang, Y., Chen, Y., Hu, K., Yang, W., Zuo, S., Xu, J., Kang, Z., Xiao, X., Li, G., 2022. A high-quality genome of *Rhizoctonia solani*, a devastating fungal pathogen with a wide host range. Mol. Plant Microbe Interact. 35, 954–958. https://doi.org/10.1094/MPMI-06-22-0126-A.

Yuan, B., Shen, X., Li, X., Xu, C., Wang, S., 2009. Pathogen-induced expressional loss of function is the key factor in race-specific bacterial resistance conferred by a recessive R gene xa13 in rice. Plant Cell Physiol. 50, 947–955. https://doi.org/10.1093/pcp/pcp046.

Zakharova, A.A., Efimova, S.S., Ostroumova, O.S., 2025. State of the art of cyclic lipopeptide–membrane interactions: pore formation and bilayer permeability. Pharmaceutics 17, 1142. https://doi.org/10.3390/pharmaceutics17091142.

Zhou, L., Höfte, M., Hennessy, R.C., 2024. Does regulation hold the key to optimizing lipopeptide production in *Pseudomonas* for biotechnology? Front. Bioeng. Biotechnol. 12, 1363183. https://doi.org/10.3389/fbioe.2024.1363183.